



ISSN: 2785-2997

Journal of Human, Earth, and Future

Vol. 2, No. 4, December, 2021



Fabrication and Characterization of p-Cu₂O on n-TiO₂ Layer by Electrodeposition Method for Heterojunction Solar Cells Development

Ahmad Norazlina^{1, 2*}, Mohamad Fariza^{1, 2}, Talib Azman^{1, 2}, Ahmad Mohd Khairul^{1, 2},
Mohd Ismail Anis Zafirah^{1, 2}, Mohamad Arifin Nurliyana^{1, 2}

¹ Department of Electrical and Electronic Engineering, Politeknik Mersing Johor, Universiti Tun Hussein Onn Malaysia, 86400, Parit Raja, Batu Pahat, Johor, Malaysia

² Microelectronics and Nanotechnology Shamsuddin Research Centre (MiNT-SRC), Universiti Tun Hussein Onn Malaysia, 86400, Parit Raja, Batu Pahat, Johor, Malaysia

Received 19 September 2021; Revised 18 November 2021; Accepted 23 November 2021; Published 01 December 2021

Abstract

This study focused on the copper (I) oxide (Cu₂O) that serves as an absorber layer, owing to its excellent optical properties, while titanium dioxide (TiO₂) is a well-known material that has superior properties in solar cell development. In this work, the TiO₂ nanorods layer was synthesised on a fluorine-doped tin oxide (FTO) glass substrate by a facile hydrothermal method followed by stacking the Cu₂O layer using a low-cost electrodeposition method at different deposition times. Prior to deposition, a cyclic voltammetry (CV) measurement was performed, and the result showed that Cu₂O films were successfully grown on the TiO₂ nanorods layer with high uniformity. The crystallinity of the Cu₂O/TiO₂ film was increased when the deposition time was elevated. The strongest diffraction peak was detected in the sample deposited for 90 minutes. FE-SEM images revealed the formation of the pyramidal structure of Cu₂O on the TiO₂ nanorod layer. The optical properties showed that the samples deposited at 60 minutes and above were red-shifted, with the estimated bandgap being slightly decreased when extending the deposition time. Meanwhile, the resistivity and sheet resistance of the as-prepared samples were increased. The performance of the solar cell was investigated, and the power energy conversion was slightly increased to 0.0267% for the heterojunction sample deposited at 90 minutes.

Keywords: Copper (I) Oxide (Cu₂O); Titanium Dioxide (TiO₂); Hydrothermal; Electrodeposition Method; Deposition Time; Heterojunction Solar Cell.

1. Introduction

The development of p-n heterojunction by coupling metal oxide semiconductor specifically p-Cu₂O with n-TiO₂ can extend the light absorption of TiO₂ toward the visible light, and the built-in intrinsic electric field originated from p-Cu₂O/n-TiO₂ heterojunction will accelerate the charge separation of photo-induced electron-hole pairs [1]. Because of these features, p-Cu₂O/n-TiO₂ heterojunction possesses prominent benefits in many application fields, such as photocatalyst either in pollutant degradation [2] or hydrogen production [3, 4] and solar energy conversion in photovoltaic devices [5]. Significant effort has been devoted to the fabrication of p-Cu₂O/n-TiO₂ heterojunctions with different hybrid or bi-layer morphologies combinations with several main purposes: (i) enhance the adsorption ability; (ii) enlarge the absorbance of light in the visible region; and (iii) favour the separation of photoinduced carriers.

* Corresponding author: azlina78.ahmad@gmail.com

<http://dx.doi.org/10.28991/HEF-2021-02-04-02>

➤ This is an open access article under the CC-BY license (<https://creativecommons.org/licenses/by/4.0/>).

© Authors retain all copyrights.

It was reported that the TiO₂ nanorod structure could provide direct conductive pathways and minimize electron-hole recombination [6]. The energetic electrons excited by visible light can be transferred to TiO₂ from the narrow bandgap semiconductor, which favours charge separation. Optimizing an appropriate semiconductor and constructing high-quality interfaces with TiO₂ would be critical for the high performance of the fabrication of heterojunction thin films. Cu₂O as a p-type semiconductor owns a narrow bandgap is expected could enhance the solar absorption, beneficial band gap and good rectification properties; such these characteristics are very useful in contributing to the high performance of the thin film.

Several studies demonstrated the development of Cu₂O/TiO₂ p-n junctions as future candidate solar cells. However, the efficiency is still low and the best result was far away from the 20% of Cu₂O theoretical limit [7–9] and 11% of TiO₂ in dye-sensitized solar cells (DSSC) application [10]. According to Hussain et al., the lower efficiency of Cu₂O/TiO₂ heterojunction film is caused by the p-n junction interface defects, large lattice mismatch, rapid electron and hole pairs recombination rate and band discontinuity [5, 11]. At the p-n junction interface, there were carrier's traps and a place for rapid recombination event. Such barriers lead to a decrease in photogenerated carrier's performance as the electrons and holes could lose their energies in the trapped path thus increases the recombination rate. As reported by Li et al. in their study, poor efficiency of Cu₂O/TiO₂ radial p-n junctions was attributed by a lower open-circuit voltage (V_{oc}) resulted from the fluctuation of reverse saturation current and shunt resistance due to the defects at the junction interface [12].

From the past studies regarding the Cu₂O/TiO₂ fabrication heterojunction films, it can be suggested that the p-n junction interfacial state is a predominant factor in determining the efficiency of photovoltaic performance. The barriers at the interface junctions should be minimized to ensure the transportation of carriers are facile and smooth. In this work, time deposition is manipulated to synthesis the Cu₂O on TiO₂ nanorods layer to investigate the carrier transportation behaviour at the p-n junction interface. In addition, CV measurement was conducted in order to investigate the influence of Cu₂O time deposition onto the TiO₂ layer.

2. Experimental Details

2.1. Preparation of TiO₂ Nanorods

All the chemicals were analytical grade and used without further purification. Fluorine-doped SnO₂ (FTO) glass (7 Ω/sq.) with a thickness of 2.0 mm was cut into the pieces of 15×25 mm in dimension as substrates. These substrates were cleaned ultrasonically in acetone followed by ethanol and lastly deionized water for 10 minutes, respectively. In a typical synthesis, 60 mL of deionized water and 60 mL of concentrated hydrochloric acid (36.5 – 38% by weight) was magnetically stirred for 5 minutes. Then, 3 mL of titanium (IV) butoxide (TBOT) was added dropwise and stirred for another 10 minutes until the colour changed from cloudy to clear without any formation of precipitation. The mixture solution was poured into a Teflon-lined autoclave where the FTO substrates were placed against the Teflon wall with an active side facing downward. The autoclave was sealed completely and hydrothermally treated for 8 hours at temperature 150 °C. After cooling down to ambient temperature, the substrates were taken out, rinsed extensively with deionized water and allowed to dry naturally in ambient air.

2.2. Preparation of Cu₂O film on TiO₂ Nanorods

Cu₂O thin films are potentiostatically electrodeposited onto TiO₂ thin film at 30, 60, 90 and 120 minutes that abbreviated as samples A, B, C and D, respectively using a standard three electrodes electrodeposition method. The TiO₂ nanorods employed as a working electrode (WE), platinum (Pt) sheet as a counter electrode (C_E) and Ag/AgCl (saturated with KCl) as reference electrodes (RE). The electrodeposition was carried out using an electrochemical test system (Solartron analytical, 1280C) under constant current and charge. An aqueous solution containing 0.4M copper (II) acetate monohydrate (Cu(Ac)₂·H₂O, Kanto Chemical Co. Inc., purity: 99.0%) and 3.0M lactic acid (CH₃CH(OH)COOH, Kanto Chemical Co. Inc., 85.0 – 92.0%) solution at a bath temperature of 60 °C as shown in Figures 7 and 8, respectively. The electrodeposition potential was –0.4 V and pH 12.5 was adjusted with the help of 4M potassium hydroxide (KOH, Kanto Chemical Co. Inc., purity: 86.0%) [13]. After the deposition took place, the sample was rinsed with deionized water to remove the remaining chemical solutions, dried in air. The experiment was carried out using a freshly prepared solution for each deposition to ensure that the reaction is mainly due to electroreduction of Cu²⁺, Cu(OH) and water producing Cu₂O film [14].

2.3. Characterization Techniques

The crystal structure of the as-synthesized films was examined by PANanalytical X-Pert³ Powder X-ray diffraction (XRD) with CuKα radiation (λ) 1.5406 Å in the Bragg angle ranging from 20 to 80° at a scanning speed of 2°min⁻¹ and the type of slit used was fixed divergence slit. The X-ray tube voltage and current were set at 40 kV and 40 mA, respectively. The morphology and microstructure of the samples were examined by field emission scanning electron microscopy (FE-SEM, JOEL, JSM-7600F). The absorbance spectra were recorded in a range of 300 – 800 nm on a UV–

Vis spectrophotometer (Shimadzu-UV 1800) to find the wavelength absorption. The 4-Point Probe (Signatone Pro4-440N) is connected to a Keithley 2420 source meter to determine the resistivity properties of the samples. The topology properties were performed by Park System XE-100 AFM from Korea. In order to complete the solar cell circuit, the $\text{Cu}_2\text{O}/\text{TiO}_2$ p-n heterojunction samples were deposited with gold as a metal contact. The photovoltaic properties were quantified by a computer-programmed Keithley 2420 source meter under simulated AM1.5G irradiation by Newport Oriel solar simulator ($100 \text{ mW}/\text{cm}^2$)

3. Results and Discussion

3.1. CV Measurement

The voltammogram for p- Cu_2O as shown in Figure 1 was yielded between + 0.5 and - 1.0 V vs. Ag/AgCl at a scan rate of 5 mV/s. However, the potential of 0 to -1.0 V was emphasised since the reduction process occurred here. The voltammogram obtained shows a negatively swept scanning with the first peak of reduction occurred at a small current density. Such a small current suggests that the Cu_2O nanocrystalline is easier to stack on the TiO_2 nanorods layer and promote a uniform growth. The deposition potential window obtained from the voltammogram was found to be - 0.33 to - 0.68 V vs. Ag/AgCl and this is consistent with the previous literature for identical electrolytes [15, 16].

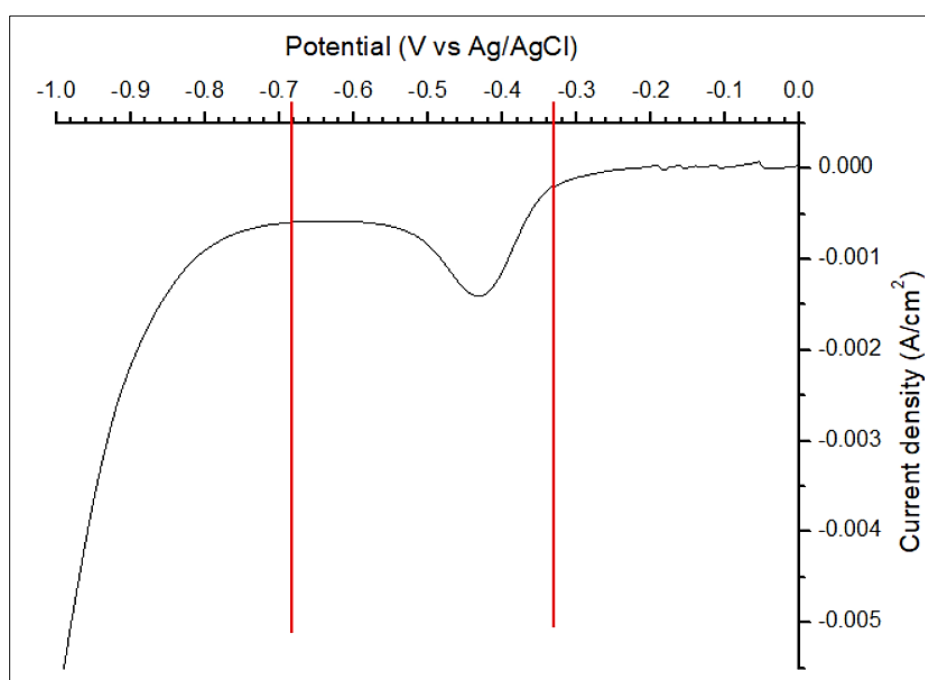


Figure 1. CV graph of Cu_2O growth on TiO_2 nanorods layer

3.2. Structural Properties

Figure 2 represents the XRD diffraction pattern of p- $\text{Cu}_2\text{O}/\text{n-nanorods-TiO}_2/\text{FTO}$ glass substrate at different Cu_2O deposition times with the sample TiO_2 nanorods serving as the reference for diffraction substrate. All the diffraction peaks that emerged in the samples are in good agreement with Cu_2O diffraction pattern of JCPDS No.05-0667 [17] and JCPDS No. 65-3288 [18]. The diffraction peaks of Cu_2O at 2θ values of 29.7° , 36.4° , 42.3° , 61.5° , 73.7° , and 77.7° that were indexed to (110), (111), (200), (220), (311) and (222) planes, respectively. Meanwhile, the rutile TiO_2 peaks could be observed and are consistent with the ones reported by Jithin and co-workers (JCPDS No: 75-1750) [19]. No other impurities such as Cu, CuO , and $\text{Cu}(\text{OH})_2$ were detected on the diffraction pattern. For the sample A that was deposited at 30 minutes, five out nine peaks corresponding to Cu_2O emerged at 29.7° , 36.4° , 42.3° , 61.5° , 73.7° , and 77.7° , that can be matched to (110), (111), (200), (220), (311), and (222) planes, respectively. In addition, three peaks corresponding to rutile TiO_2 were detected at $2\theta = 36.7^\circ$, 54.5° , and 70° , which corresponded to (101), (211), and (301) planes, respectively. However, these peaks low and weak intensity, which indicates that Cu_2O did not fully grow on the TiO_2 nanorods layer.

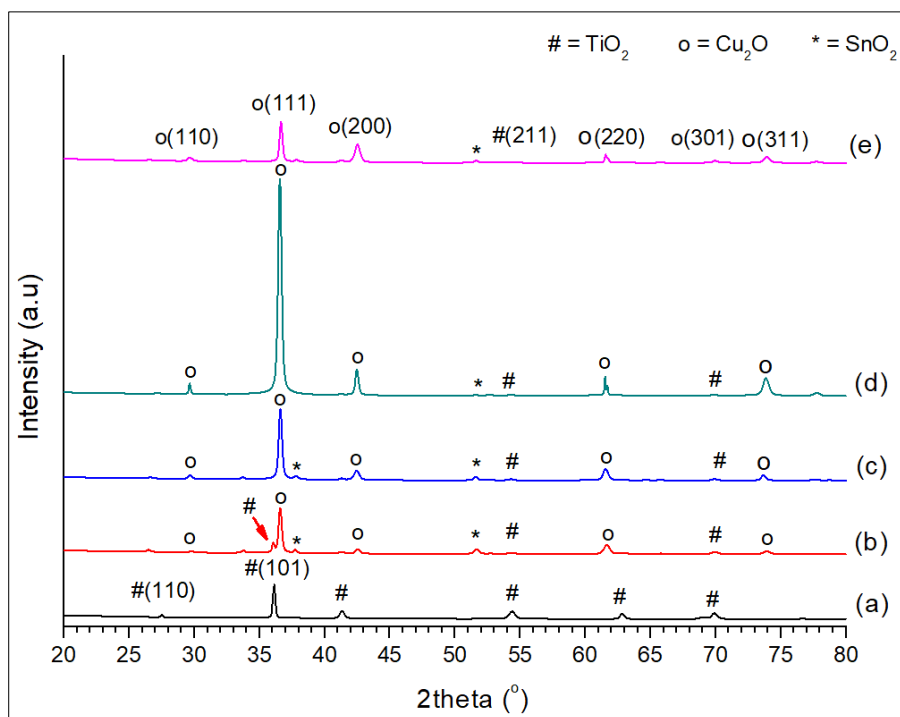


Figure 2. XRD diffraction patterns of samples (a) TiO₂ nanorods and Cu₂O deposition for (b) 30, (c) 60, (d) 90, and (e) 120 minutes

Increasing the deposition time to 60 minutes that refers to sample B, resulted in the disappearing of commonly intensive rutile TiO₂ peak located at $2\theta = 35.7^\circ$ assigned to (101) plane, suggesting that the entire TiO₂ layer was fully encompassed by Cu₂O layer. Moreover, one emergence of new Cu₂O peak at $2\theta = 77.7^\circ$ matched to (222) plane indicates the highly and purely crystalline of thin-film synthesised. Elevating the deposition time to 90 minutes as represented by sample C, the strongest and highest diffraction peak was detected at 2θ value of 36.5° , which corresponded to Cu₂O at (111) plane. By increasing the deposition time to 120 minutes (sample D), the peak intensity of Cu₂O dramatically decreased attributed by too much Cu₂O nanocrystalline was loaded into the TiO₂ structure due to the prolonged deposition duration. The preferred orientation corresponding to the plane (111) of Cu₂O was observed and identified as the highest intense peak in all of the samples but most prominent in the sample deposited for 90 minutes (sample C).

The crystallite size of Cu₂O phase was calculated by Scherrer equation [20]. It can be observed that the crystallite sizes of Cu₂O increased when the deposition time increased as proven by the FWHM values as shown in Table 1. The crystallite size of Cu₂O deposited for 30 minutes was found to be 32.49 nm. Further elevated the deposition time to 60 minutes, enlarged the Cu₂O crystallite size to 35.17 nm. Keep rising the deposition time of 90 minutes, the Cu₂O crystallite size rose to 38.06 nm, and the size was extended to 41.47 nm when the deposition time of 120 minutes was employed.

Table 1. Structural parameters of Cu₂O/TiO₂ nanorods/FTO with different Cu₂O deposition time calculated from XRD patterns

Sample	Deposition time (minutes)	2θ (°)	FWHM, β	Crystallite size, D (nm)	Plane (h,k,l)
A	30	36.55	0.2640	32.49	111
B	60	36.56	0.2755	35.17	111
C	90	36.65	0.2558	38.06	111
D	120	36.62	0.2362	41.47	111

3.3. Surface Morphology

The surface morphologies of Cu₂O/nanorods-TiO₂/FTO heterostructure thin film yielded at different deposition times from the same bath solution containing 0.4 M Cu(Ac)₂ and 3 M lactic acid which adjusted to pH 12 by KOH, are shown in Figure 3. It was revealed that truncated cubic and 3-sided pyramidal particles made up the deposits formed at 30, 60, 90, and 120 minutes, which are typically found in general formation of Cu₂O film. For sample A that was deposited for 30 minutes, the Cu₂O layer was distributed unevenly, which indicates that such duration is inadequate time for uniform distribution of Cu₂O, since the uniformity is very crucial for enhancing electron transportation. The diameter of the particles was estimated to be around 0.2 to 0.7 μm . Moreover, the TiO₂ nanorods structure was obviously noticed in the FE-SEM images as depicted in Figure 3-a and this is confirmed by the detection of the rutile TiO₂ phase in the XRD diffraction pattern.

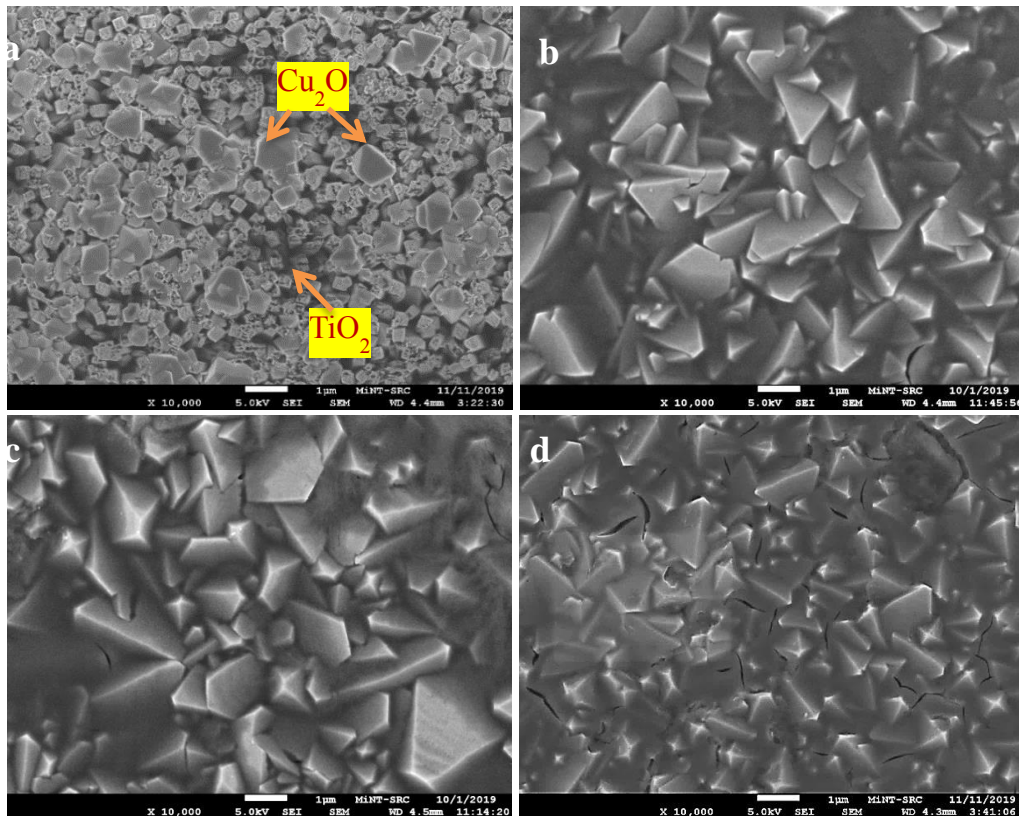


Figure 3. FE-SEM images of the Cu₂O deposited at (a) 30, (b) 60, (c) 90 and (d) 120 minutes on TiO₂ nanorods sample under x 10,000 magnification, respectively

A clear transformation of Cu₂O truncated cubic particles to 3-sided pyramidal structure could be observed when the deposition time continues to 60 minutes, as shown in Figure 3-b. It was exhibited that the pyramid structure was encompassed and distributed evenly on the TiO₂ nanorods layer. The diameter of Cu₂O particles enlarged and was estimated to be 0.7 to 1.3 μm. By extending the deposition time to 90 minutes, a structure resembling the sample deposited at 60 minutes was obtained. Such pyramidal structure became bigger with an estimated diameter of 0.8 to 2.5 μm. It also could be noticed that some of the pyramid growth formed a flaky structure as shown in Figure 3-c. After prolonging the electrodeposition process to 120 minutes, an ambiguous pyramid structure was exhibited as depicted in Figure 3-d. This structure is apparently embedded in a flaky sheet of Cu₂O. However, the diameter of the particles deposited at 120 minutes was dramatically reduced to be in the range of 0.6 to 1.2 μm. Therefore, it can be suggested that elongated electrodeposition time is beneficial for a uniform growth of Cu₂O; however, if it is conducted for a longer period, it will slowly hinder the Cu₂O enlargement and this may be attributed to the decrease of the growth rate reaction.

From the cross-sectional images as shown in Figure 3, the thickness of Cu₂O/ nanorods-TiO₂/FTO heterostructure thin film was expected to exceed more than 3 μm. This is because the initial thickness of hydrothermally grown TiO₂ nanorods film was estimated 3.00 μm. For the sample deposited in 30 minutes, the Cu₂O pyramidal structure was difficult to observe. The formation of Cu₂O was distributed unevenly on the TiO₂ layer and the thickness was found to be 3.13 μm. By continuing the electrodeposition time to 60 minutes exhibited an increment in the thickness, which was 3.18 μm. The pyramid structure could be seen clearly, which indicates that uniform of Cu₂O distribution has been achieved. Increasing the time to 90 minutes reveals that the Cu₂O was filled-in the gap between the adjacent nanorods. A film thickness of 3.28 μm was achieved when the deposition time was elongated to 90 minutes. Elevating the time to 120 minutes increased the film thickness to 3.50 μm. In this stud, the electrodeposition process was conducted at high pH level which is 12, and high solution temperature of 60 °C. Increased deposition time is favourable in increasing the film thickness as reported by a previous study [21].

3.4. Optical Properties

Figure 4 shows the UV-Vis spectra of the heterojunction samples Cu₂O/TiO₂ nanorods at different electrodeposition times. Considering the TiO₂-nanorods served as the reference sample, the distinction pattern of light absorbance could be traced easily. From the spectra, it can be noticed that the Cu₂O deposited at 30 minutes on the TiO₂-nanorods layer showed the absorption through the entire UV and visible light region. This is attributed to the uneven distribution of Cu₂O on TiO₂ nanorods structure, which enabled the light source to pass through both materials as confirmed by XRD diffraction pattern and FE-SEM image. However, the samples deposited at 60, 90, and 120 minutes exhibited a stronger absorption at visible light region which could be attributed by more Cu₂O nanoparticles that were loaded into the space between the etched nanorods structure. Increasing the deposition time was resulted more light absorption, but too much Cu₂O deposited could lead to high reflection and lowering the light penetration into TiO₂ nanorods structure.

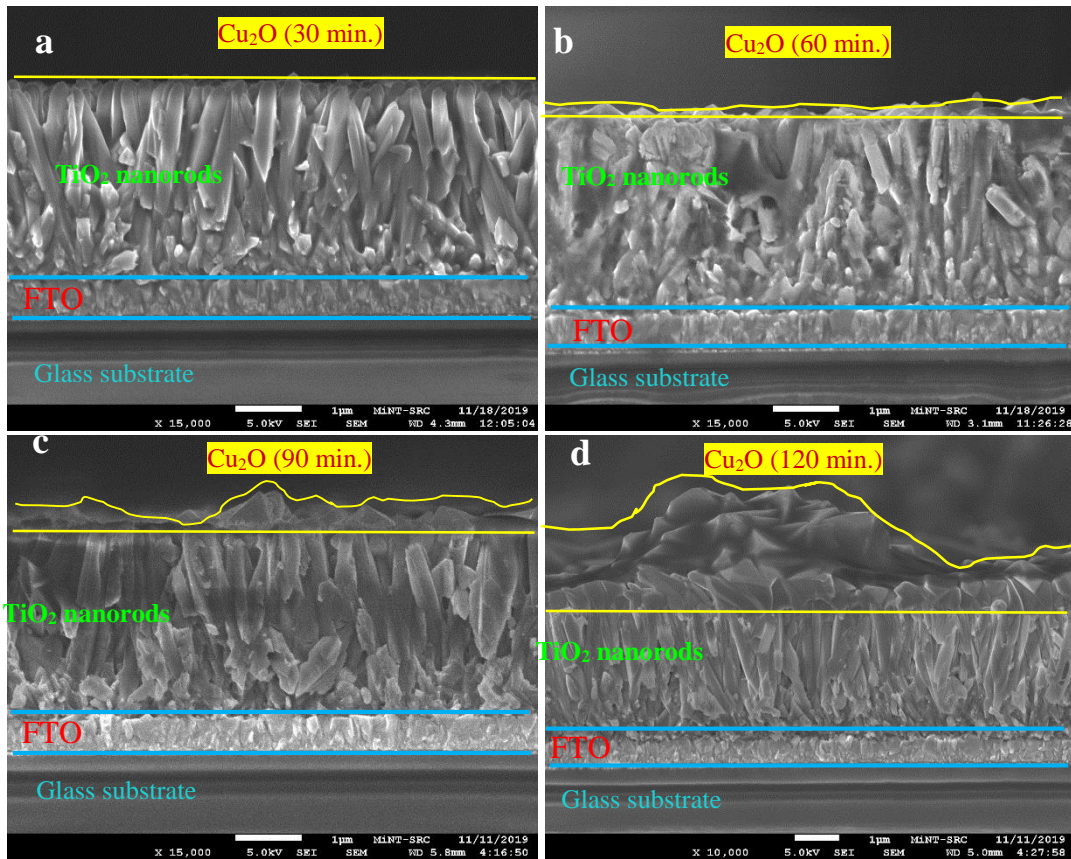


Figure 4. FE-SEM images of the cross-sectional images after Cu₂O deposited for (a) 30, (b) 60, (c) 90, and (d) 120 minutes onto TiO₂ nanorods layer

Figure 5 displays the UV-vis transmittance spectrum of the as-prepared samples. It can be seen that the 30 minutes of grown Cu₂O fell in the red-shift region, which indicates that the TiO₂ nanorods structure in this sample is exposed to the light due to the uneven distribution of Cu₂O. However, elevating the time of Cu₂O deposition to 60, 90, and 120 minutes shifted the spectrum towards the blue regions suggesting more light at the visible region could be transmitted to the nanorods TiO₂ layer.

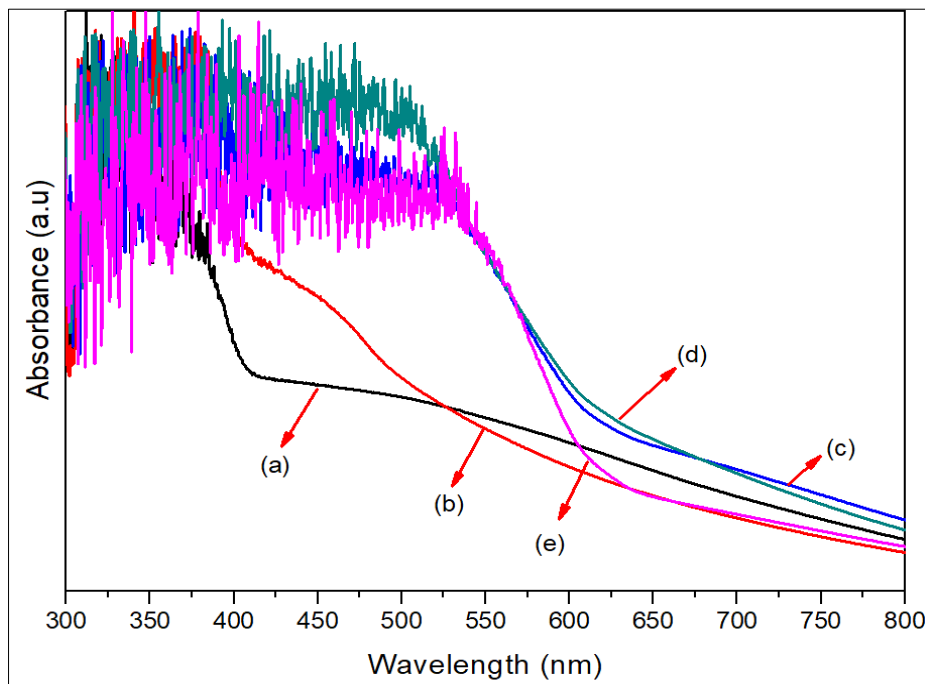


Figure 5. Absorption spectra of (a) TiO₂ sample and Cu₂O electrodeposition time at (b) 30, (c) 60, (d) 90 and (e) 120 minutes

Figure 6 displays the UV-vis transmittance spectrum of the as-prepared samples. It can be seen that the 30 minutes of grown Cu_2O falls in the redshift region indicates that the TiO_2 nanorods structure in this sample is exposed to the light due to the uneven distribution of Cu_2O . However, elevating the time of Cu_2O grown to 60, 90 and 120 minutes shifted the spectrum towards the blue regions suggesting more light at the visible region could be transmitted to the nanorods TiO_2 layer.

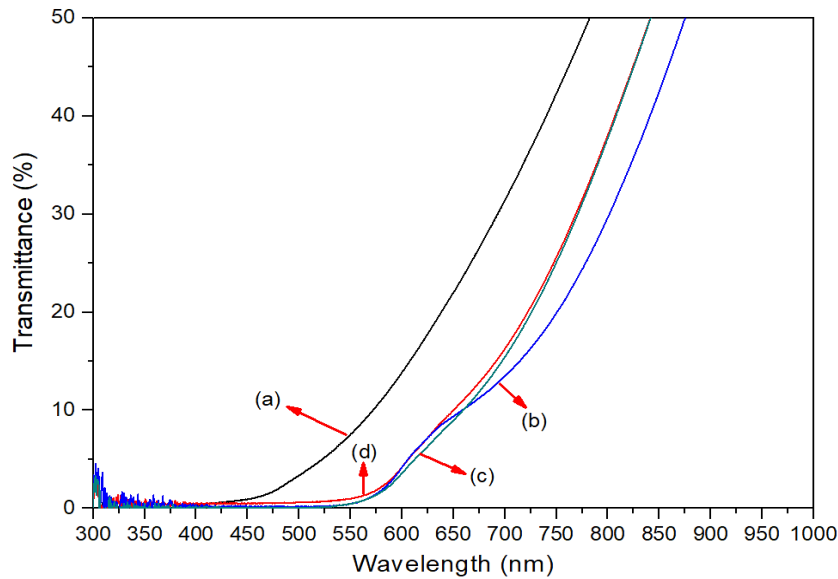


Figure 6. Transmittance spectra of $\text{Cu}_2\text{O}/\text{TNR}_{\text{Etch-5}}$ film at different deposition time of (a) 30, (b) 60, (c) 90 and (d) 120 minutes

The bandgap may be derived from the optical absorption (α) by extrapolating a linear fit to the plot $(\alpha h\nu)^2$ versus $h\nu$ to zero as illustrated in Figure 7. The band gaps obtained are 2.10, 1.90, 1.90 and 1.91 eV for 30, 60, 90 and 120 minutes of Cu_2O deposition, respectively. These values are slightly lower than the normally reported of 2.17 eV [22]. However, the sample deposited at 120 minutes showed more surface roughness, which contributes to a wider band gap, attributed to the effect of light scattering during measurement recorded [23].

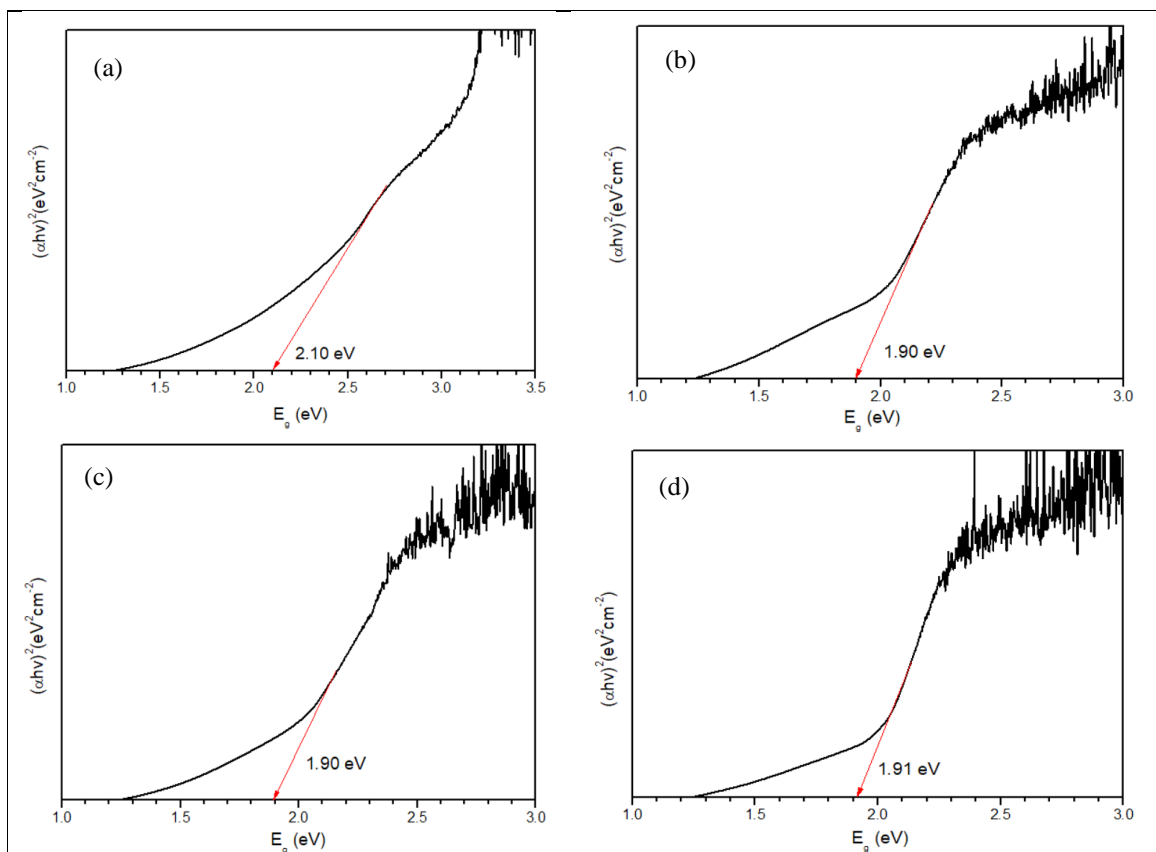


Figure 7. Estimated band gap for as-prepared samples at different deposition time of (a) 30, (b) 60, (c) 90 and (d) 120 minutes

3.5. Topology Properties

The surface topology images of the Cu₂O films deposited at different times on nanorods TiO₂ were studied through 3D AFM images. The RMS roughness of the Cu₂O/ TiO₂-nanorods-/FTO samples were found to be 63.4, 74.6, 91.1, and 126.8 nm for the sample deposited at 30, 60, 90, and 120 minutes, respectively. Meanwhile, the 3D images can be observed in Figure 8. The roughness is in an increasing pattern, suggesting that the deposition duration affected the roughness of Cu₂O growth. It can be clearly observed that at 30 minutes of electrodeposition, the roughness of deposited Cu₂O was slightly low, which indicates less uniformity of Cu₂O layer. Increasing the deposition time increased the uniformity growth of the Cu₂O layer, in which the roughness were found to be 74.6, 91.1, and 126.8 nm for the sample deposited at 60, 90, and 120 minutes, respectively. From the result attained, it can be inferred that the RMS roughness of Cu₂O/TiO₂-nanorods-/FTO increases as the deposition time increases, due to the fluctuating shape of the pyramid structure, attributed to adequate time for Cu₂O growth as confirmed by FE-SEM images.

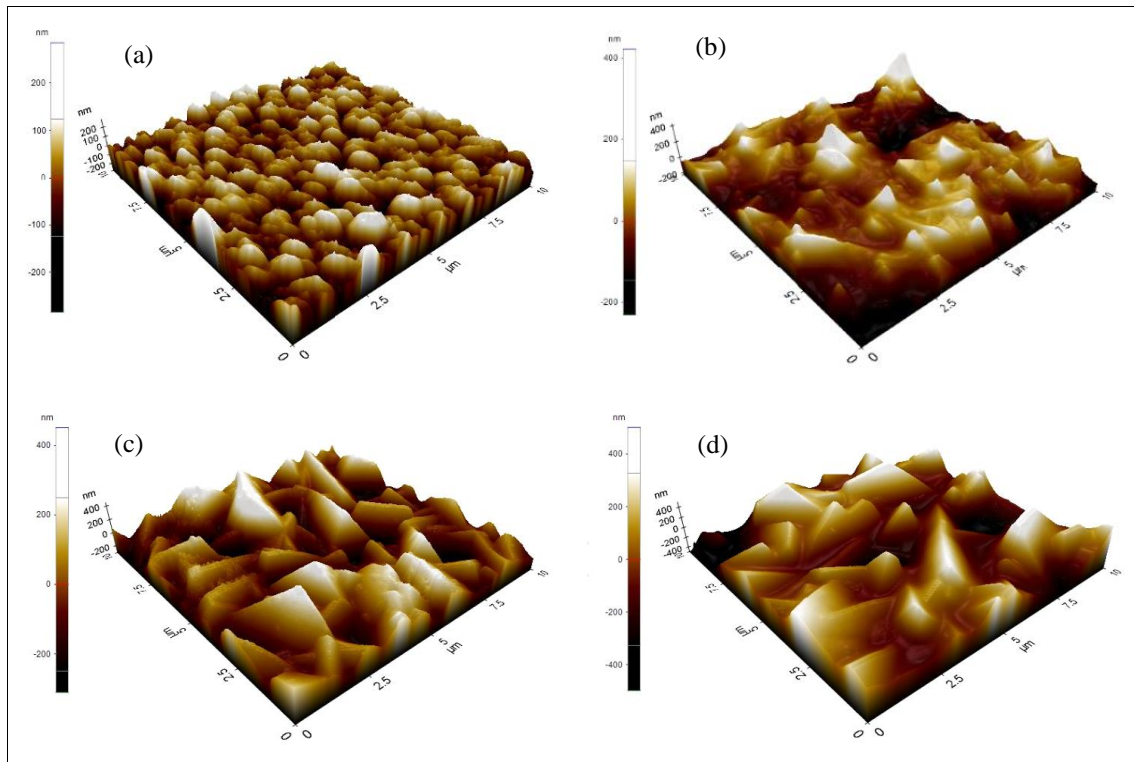


Figure 8. AFM images of the Cu₂O films obtained at different electrodeposition time of (a) 30, (b) 60, (c) 90 and (d) 120 minutes on nanorods TiO₂ structure

3.6. Electrical Properties

To investigate the electrical properties of the Cu₂O/nanorods-TiO₂/FTO film, the samples were characterised by four-point probe, a typical measurement tool to determine the resistivity, ρ and sheet resistance, R_s of the film synthesised through the thickness of the film. From the result obtained as shown in Table 2, the ρ and R_s of the Cu₂O/nanorods-TiO₂/FTO film showed an increasing pattern as the time for electrodepositing increased. The increment behaviour is attributed to rapid growth rate of Cu₂O and accelerated from the beginning of the electrodeposition as early as 30 minutes. Expanding the time deposition boosted the growth rate thus increased the film thickness, simultaneously increasing the resistivity and sheet resistance of Cu₂O/TiO₂-nanorods/FTO film.

Table 2. Electrical properties of as-prepared samples synthesized at different deposition time

Sample	Deposition time (minutes)	Resistivity, ρ (Ω .cm)	Sheet resistance, R_s ($\times 10^3 \Omega$ /sq.)	Film thickness (μ m)
A	30	11.92	39.74	3.13
B	60	14.40	46.15	3.18
C	90	17.43	53.15	3.28
D	120	19.41	55.47	3.50

The efficiency of the TiO₂ films is determined under simulated sunlight at 100 mW/cm² and summarised in Table 3. The open-circuit voltages (V_{oc}) for samples deposited at 30, 60, 90, and 120 minutes are 286.9, 342.3, 420.1, and 205.9

mV, respectively. The fluctuation of values indicates the internal electric field is unstable and this might be attributed to the defects at the junction interface, which is caused by continuous deposition for 120 minutes and poor adhesion of metal contact on Cu₂O film. However, the short-circuit current density (J_{sc}) for samples A, B and C is dramatically increased from 0.0287, 0.0394 and 0.1978 mA/cm², respectively before gradually decreasing to 0.0271 mA/cm² for samples deposited at 120 minutes. The fill factors (FF) increased from 19.70 and 60.91 before drop to 32.08 and finally to 29.09 for the samples deposited at 30, 60, 90 and 120 minutes of electrodeposition time. Therefore, the power energy conversion efficiency was deduced to be 0.0016%, 0.0082%, 0.0267%, and 0.0015% for the samples. From the results, the sample deposited at 90 minutes showed an improvement which yielded 0.0267% of power energy conversion. However, the result is far from the theoretical value of Cu₂O solar cell, which is 20% of power energy conversion.

Table 3. Photovoltaic parameters of the as-prepared samples

Sample	Deposition time (minutes)	V_{oc} (mV)	J_{sc} (mA/cm ²)	FF (%)	η (%)
A	30	286.9	0.0287	19.70	0.0016
B	60	342.3	0.0394	60.91	0.0082
C	90	420.1	0.1978	32.08	0.0267
D	120	205.9	0.0271	29.09	0.0015

A schematic representation of the charge transfer mechanism in the TiO₂ nanorods with Cu₂O layer in thin film solar cell under irradiation is presented in Figure 9. The energetic electrons in Cu₂O is excited from the valance band (VB) to the conduction band (CB), whereas the holes generated on the VB of TiO₂ diffuses to the Cu₂O. This photoexcited charge transfer can be remarkably intensified by an inner electric field built at the interface of TiO₂ and Cu₂O. The combination of the inner electric field and intrinsic energy band gap nature promotes efficiently separation of photogenerated electrons and holes, simultaneously reducing the chances of electron-hole pair recombination. The separated electrons on the CB of TiO₂ flow through the FTO and arrive at the gold contact to combine with the hole again.

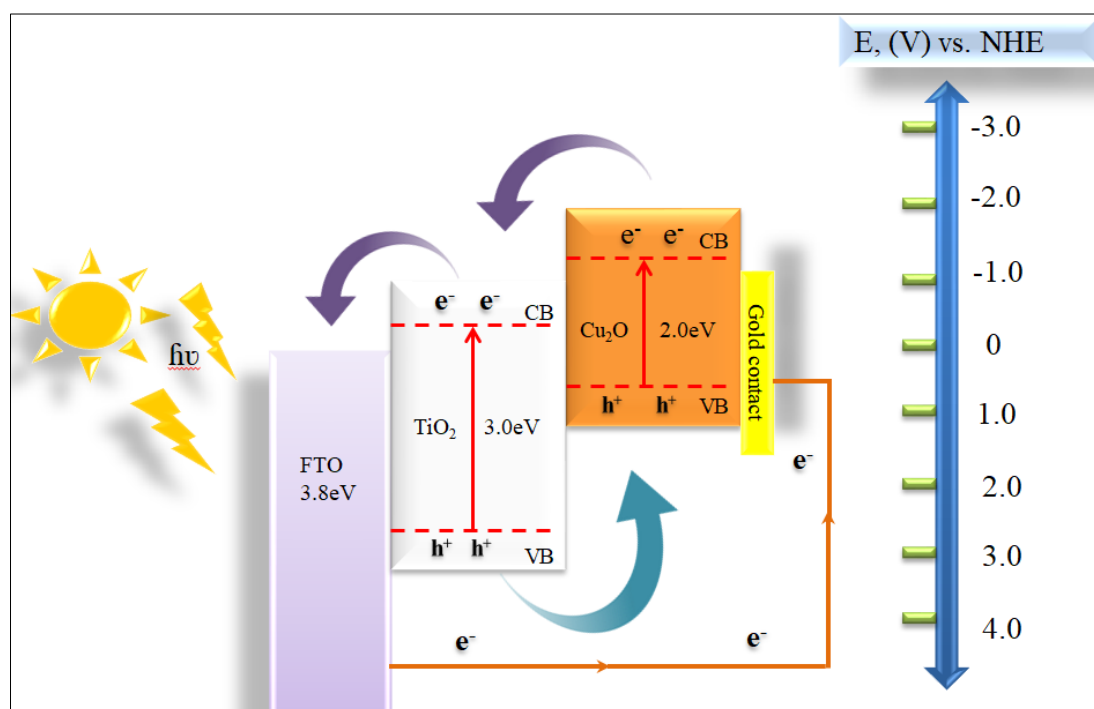


Figure 9. Schematic mechanism of the charge transfer mechanism in Cu₂O-TiO₂ system on irradiation

4. Conclusion

One series of TiO₂ nanorods samples with a thickness of 3 μ m were prepared to investigate the effect of Cu₂O time deposition. The duration was manipulated from 30, 60, 90, and 120 minutes. The crystallinity of the Cu₂O/TiO₂ film increased when the deposition time was elevated. The strongest diffraction peak was detected in the sample deposited for 90 minutes, with a crystallite size of 35.7 nm. FE-SEM images reveal that 60 minutes and above was adequate time for depositing the Cu₂O layer evenly on the TiO₂ nanorods layer. Only samples deposited at 60 minutes and above were red-shifted, as proven by optical absorbance analysis. The estimated band gap slightly decreased when deposition time

was extended. Meanwhile, the resistivity and sheet resistance of the as-prepared samples increased. The performance of the solar cell was investigated, and the power energy conversion slightly increased to 0.00267% for the Cu₂O/TiO₂ heterojunction sample deposited at 90 minutes. Although the power conversion is below the theoretical limit, this work would inspire the other researchers to do more intensive investigations specifically into Cu₂O-based heterojunction in various fields of applications.

5. Declarations

5.1. Author Contributions

Conceptualization, A.N. and M.F.; methodology, A.N.; software, T.A.; validation, A.M.K. and M.F.; formal analysis, M.I.A.Z.; investigation, A.N.; resources, M.F. and A.M.K.; data curation, A.N.; writing—original draft preparation, A.N.; writing—review and editing, M.F.; visualization, A.M.K.; supervision, M.F.; project administration, M.A.N.; funding acquisition, A.N., M.F. and A.M.K. All authors have read and agreed to the published version of the manuscript.

5.2. Data Availability Statement

The data presented in this study are available in article.

5.3. Funding and Acknowledgements

The authors would like to acknowledge Fundamental Research Grant Scheme (FRGS) vot. K188 (Ref. No: FRGS/1/2019/TK10/UTHM/02/3) and Program Hadiah Latihan Persekutuan (HLP 2017/2018) from Ministry of Higher Education Malaysia. Special thanks to Microelectronic and Nanotechnology – Shamsuddin Research Centre (MiNT-SRC) and Universiti Tun Hussein Onn Malaysia for the facilities provided as well as the colleagues and expertise from the technical support team.

5.4. Institutional Review Board Statement

Not applicable.

5.5. Informed Consent Statement

Not applicable.

5.6. Declaration of Competing Interest

The authors declare that there is no conflict of interests regarding the publication of this manuscript. In addition, the ethical issues, including plagiarism, informed consent, misconduct, data fabrication and/or falsification, double publication and/or submission, and redundancies have been completely observed by the authors.

6. References

- [1] Fei, X., Li, F., Cao, L., Jia, G., & Zhang, M. (2015). Adsorption and photocatalytic performance of cuprous oxide/titania composite in the degradation of acid red B. *Materials Science in Semiconductor Processing*, 33, 9–15. doi:10.1016/j.mssp.2015.01.022.
- [2] Ma, Q., Zhang, H., Cui, Y., Deng, X., Guo, R., Cheng, X., Xie, M., & Cheng, Q. (2018). Fabrication of Cu₂O/TiO₂ nano-tube arrays photoelectrode and its enhanced photoelectrocatalytic performance for degradation of 2,4,6-trichlorophenol. *Journal of Industrial and Engineering Chemistry*, 57, 181–187. doi:10.1016/j.jiec.2017.08.020.
- [3] Kavitha, S., Jayamani, N., & Barathi, D. (2020). A study on preparation of unique TiO₂/Cu₂O nanocomposite with highly efficient photocatalytic reactivity under visible-light irradiation. *Materials Technology*, 36(11), 670–683. doi:10.1080/10667857.2020.1786785.
- [4] Dubey, P. K., Kumar, R., Tiwari, R. S., Srivastava, O. N., Pandey, A. C., & Singh, P. (2018). Surface modification of aligned TiO₂ nanotubes by Cu₂O nanoparticles and their enhanced photo electrochemical properties and hydrogen generation application. *International Journal of Hydrogen Energy*, 43(14), 6867–6878. doi:10.1016/j.ijhydene.2018.02.127.
- [5] Hussain, S., Cao, C., Usman, Z., Chen, Z., Nabi, G., Khan, W. S., Ali, Z., Butt, F. K., & Mahmood, T. (2012). Fabrication and photovoltaic characteristics of Cu₂O/TiO₂ thin film heterojunction solar cell. *Thin Solid Films*, 522, 430–434. doi:10.1016/j.tsf.2012.08.013.
- [6] Jiang, Y., Li, M., Song, D., Li, X., & Yu, Y. (2014). A novel 3D structure composed of strings of hierarchical TiO₂ spheres formed on TiO₂ nanobelts with high photocatalytic properties. *Journal of Solid State Chemistry*, 211, 90–94. doi:10.1016/j.jssc.2013.12.002.
- [7] Sawicka-Chudy, P., Sibiński, M., Wisz, G., Rybak-Wilusz, E., & Cholewa, M. (2018). Numerical analysis and optimization of Cu₂O/TiO₂, CuO/TiO₂, heterojunction solar cells using SCAPS. *Journal of Physics: Conference Series*, 1033(1), 0–10. doi:10.1088/1742-6596/1033/1/012002.

- [8] Naceur, K., Tibermacine, T., Mehiri, F., Boumaaraf, R., Labed, M., Meftah, A., ... Sengouga, N. (2021). Study and optimization of Cu₂O/AZO hetero-junction solar cell with different buffer layers. *Optical Materials*, 115, 111060. doi:10.1016/j.optmat.2021.111060.
- [9] Mitroi, M. R., Ninulescu, V., & Fara, L. (2017). Performance Optimization of Solar Cells Based on Heterojunctions with Cu₂O: Numerical Analysis. *Journal of Energy Engineering*, 143(4), 04017005. doi:10.1061/(asce)ey.1943-7897.0000431.
- [10] Boschloo, G., & Hagfeldt, A. (2009). Characteristics of the iodide/triiodide redox mediator in dye-sensitized solar cells. *Accounts of Chemical Research*, 42(11), 1819–1826. doi:10.1021/ar900138m.
- [11] Hussain, S., Cao, C., Khan, W. S., Nabi, G., Usman, Z., Majid, A., Alharbi, T., Ali, Z., Butt, F. K., Tahir, M., Tanveer, M., & Idress, F. (2014). Cu₂O/TiO₂ nanoporous thin-film heterojunctions: Fabrication and electrical characterization. *Materials Science in Semiconductor Processing*, 25, 181–185. doi:10.1016/j.mssp.2013.11.018.
- [12] Li, D., Chien, C. J., Deora, S., Chang, P. C., Moulin, E., & Lu, J. G. (2011). Prototype of a scalable core-shell Cu₂O/TiO₂ solar cell. *Chemical Physics Letters*, 501(4–6), 446–450. doi:10.1016/j.cplett.2010.11.064.
- [13] Fariza, M., Norazlina, A., Fadilah Norazni, F., Zafirah, A., Mohd Khairul, A., Azman, T., Nabihah, A., Hisyamudin Muhd Nor, N., & Izaki, M. (2019). Fabrication of Nanorods-TiO₂ for Heterojunction Thin Film Application with Electrodeposit-p-Cu₂O Absorbing Layer. *Materials Today: Proceedings*, 18, 468–472. doi:10.1016/j.matpr.2019.06.233.
- [14] Izaki, M., Sasaki, S., Mohamad, F. B., Shinagawa, T., Ohta, T., Watase, S., & Sasano, J. (2012). Effects of preparation temperature on optical and electrical characteristics of (111)-oriented Cu₂O films electrodeposited on (111)-Au film. *Thin Solid Films*, 520(6), 1779–1783. doi:10.1016/j.tsf.2011.08.079.
- [15] Izaki, M., Sasaki, S., Mohamad, F. B., Shinagawa, T., Ohta, T., Watase, S., & Sasano, J. (2012). Effects of preparation temperature on optical and electrical characteristics of (111)-oriented Cu₂O films electrodeposited on (111)-Au film. *Thin Solid Films*, 520(6), 1779–1783. doi:10.1016/j.tsf.2011.08.079.
- [16] Pagare, P. K., & Torane, A. P. (2017). Electrodeposition and characterization of pH transformed Cu₂O thin films for electrochemical sensor. *Journal of Materials Science: Materials in Electronics*, 28(2), 1386–1392. doi:10.1007/s10854-016-5672-1.
- [17] Wang, J., Ji, G., Liu, Y., Gondal, M. A., & Chang, X. (2014). Cu₂O/TiO₂ heterostructure nanotube arrays prepared by an electrodeposition method exhibiting enhanced photocatalytic activity for CO₂ reduction to methanol. *Catalysis Communications*, 46, 17–21. doi:10.1016/j.catcom.2013.11.011.
- [18] Mao, P., Liu, Y., Liu, X., Wang, Y., Liang, J., Zhou, Q., Dai, Y., Jiao, Y., Chen, S., & Yang, Y. (2017). Bimetallic AgCu/Cu₂O hybrid for the synergetic adsorption of iodide from solution. *Chemosphere*, Vol. 180, 317–325. doi:10.1016/j.chemosphere.2017.04.038.
- [19] Jithin, M., Saravanakumar, K., Ganesan, V., Reddy, V. R., Razad, P. M., Patidar, M. M., Jeyadheepan, K., Marimuthu, G., Sreelakshmi, V. R., & Mahalakshmi, K. (2017). Growth, mechanism and properties of TiO₂ nanorods embedded nanopillar: Evidence of lattice orientation effect. *Superlattices and Microstructures*, 109, 145–153. doi:10.1016/j.spmi.2017.04.046.
- [20] Ahmad, N., Mohamad, F., Ahmad, M. K., & Talib, A. (2019). Influence of growth temperature on tio₂ nanostructures by hydrothermal synthesis. *International Journal of Engineering and Advanced Technology*, 8(6 Special Issue 3), 936–941. doi:10.35940/ijeat.F1063.0986S319.
- [21] Bandara, K. N. D., Jayathilaka, K. M. D. C., Dissanayake, D. P., & Jayanetti, J. K. D. S. (2021). Surface engineering of electrodeposited cuprous oxide (Cu₂O) thin films: Effect on hydrophobicity and LP gas sensing. *Applied Surface Science*, 561, 150020. doi:10.1016/j.apsusc.2021.150020.
- [22] Chen, L. C. (2013). Review of preparation and optoelectronic characteristics BN of Cu₂O-based solar cells with nanostructure. *Materials Science in Semiconductor Processing*, 16(5), 1172–1185. doi:10.1016/j.mssp.2012.12.028.
- [23] Liu, Y. L., Liu, Y. C., Mu, R., Yang, H., Shao, C. L., Zhang, J. Y., Lu, Y. M., Shen, D. Z., & Fan, X. W. (2005). The structural and optical properties of Cu₂O films electrodeposited on different substrates. *Semiconductor Science and Technology*, 20(1), 44–49. doi:10.1088/0268-1242/20/1/007.